# Cation Recombination Energy/Coulomb Repulsion Effects in ETD/ECD as Revealed by Variation of Charge per Residue at Fixed Total Charge

Marija Mentinova[1], **David M. Crizer**[1,2], **Takashi Baba**[2], **William M. McGee**[1], **Gary L. Glish**[2], and **Scott A. McLuckey**[1]

[1]Department of Chemistry, Purdue University, West Lafayette, IN 47907-2084, USA

[2]Department of Chemistry, University of North Carolina, Chapel Hill, NC 27599, USA

Abstract
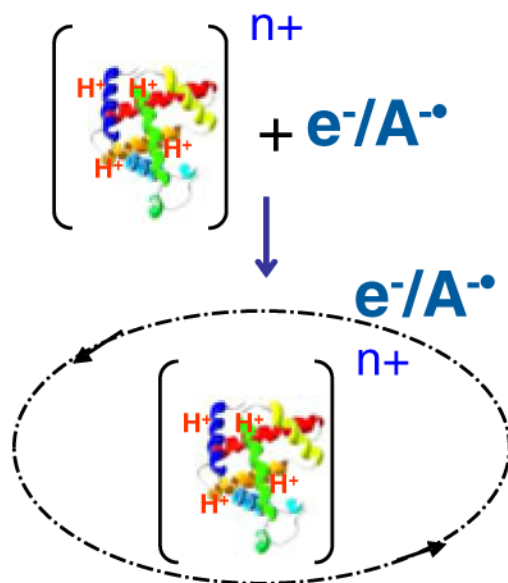
Electron capture dissociation (ECD) and electron transfer dissociation (ETD) experiments in electrodynamic ion traps operated in the presence of a bath gas in the 1–10 mTorr range have been conducted on a common set of doubly protonated model peptides of the form $X(AG)_nX$ (X = lysine, arginine, or histidine, n=1, 2, or 4). The partitioning of reaction products was measured using thermal electrons, anions of azobenzene, and anions of 1,3-dinitrobenzene as reagents. Variation of n alters the charge per residue of the peptide cation, which affects recombination energy. The ECD experiments showed that H-atom loss is greatest for the n=1 peptides and decreases as n increases. Proton transfer in ETD, on the other hand, is expected to increase as charge per residue decreases (i.e., as n increases). These opposing tendencies were apparent in the data for the $K(AG)_nK$ peptides. H-atom loss appeared to be more prevalent in ECD than in ETD and is rationalized on the basis of either internal energy differences, differences in angular momentum transfer associated with the electron capture versus electron transfer processes, or a combination of the two. The histidine peptides showed the greatest extent of charge reduction

Correspondence to: Scott A. McLuckey; mcluckey@purdue.edu.

without dissociation, the arginine peptides showed the greatest extent of side-chain cleavages, and the lysine peptides generally showed the greatest extent of partitioning into the c/z•-product ion channels. The fragmentation patterns for the complementary c- and z•-ions for ETD and ECD were found to be remarkably similar, particularly for the peptides with X = lysine.

Keywords

Electron transfer dissociation (ETD); Electron capture dissociation (ECD); Recombination energy; charge per residue

Introduction

The structural identification and characterization of peptides and proteins by mass spectrometry relies on the exposure of gas phase biomolecule ions of various types to one or more dissociation techniques [1]. Collision induced dissociation (CID) [2] is the dominant approach for the characterization of peptide and protein ions, whereas infrared multiphoton dissociation (IRMPD) [3] has been used to provide similar results. Both rely primarily on the vibrational excitation of the precursor ion. Electron capture dissociation (ECD) is one of several fragmentation techniques developed as an alternative to the vibrational activation methods, and is, instead, based on the capture of near-thermal energy electrons by multiply protonated polypeptides, resulting in dissociation [4]. The ion/ion analog to ECD is electron transfer dissociation (ETD) [5, 6]. In an electron transfer dissociation (ETD) ion/ion reaction [7–9], an electron is transferred from a reagent anion, such as the radical anions derived from fluoranthene or azobenzene, to a polypeptide cation. Upon electron transfer, the charge-reduced peptide ion undergoes fragmentation similar to ECD. In both cases, dissociation of backbone N–C and disulfide bonds is prevalent and very often gives information complementary to that derived from CID. The observed dissociation along the peptide backbone is less dependent upon peptide sequence than in CID, and is independent of the presence of CID-labile post-translational modifications (PTMs). Both ECD and ETD preserve PTMs and, as a result, enable their localization in biomolecules. This characteristic of preserving CID-labile PTMs has been offered in support for the notion that ECD and ETD are nonergodic processes [10]. However, the extent to which intramolecular energy transfer occurs in ECD/ETD remains unclear [11].

While the study of the mechanisms governing ECD and ETD is ongoing, a few mechanisms have garnered most support and attention. An early mechanistic proposal suggested electron localization at a protonated lysine (K) or arginine (R) side chain resulting in neutralization of the charge and in hydrogen atom loss [12]. In this mechanism, commonly referred to as the Cornell mechanism, the released hydrogen atom is then either transferred to a nearby carbonyl oxygen of an amide group, where it facilitates the cleavage of the N–C bond via an aminoketal radical intermediate, or to a disulfide bond, resulting in its cleavage [13, 14]. Findings of the Marshall group, who studied Lys-protonated dimers of $Ac-Cys-Ala_n-Lys$ (i.e., $[Ac-CA_nK + H]_2^{2+}$), however, suggested the possibility of an additional mechanism for the cleavage of N–C and S–S bonds [15]. A "coulomb stabilized dissociation model" (often termed the Utah-Washington model) was independently proposed by Tureček and co-workers [16], and Simons and co-workers [17, 18], who indicated that low-lying empty π^* orbitals can have their energies lowered by attractive coulomb interactions with positively charged groups (e.g., ammonium, guanidinium, or fixed charge) rendering exothermic attachment or transfer of the electron. A number of theoretical studies have been undertaken to evaluate the probability for initial placement of the electron in a Rydberg orbital of a charge site followed by subsequent transfer to an antibonding amide orbital. Early reports focused on the probabilities and cross sections for electron transfer from anion donors into

only very low-lying Rydberg orbitals on positive sites and the rates of electron transfer into SS σ* or OCN amide π* orbitals from n=3 or n=4 Rydberg orbitals on positive sites [19, 20]. More recent reports provide a more complete set of predictions about intramolecular electron transfer in ETD, given the electronic binding energy of the anion donor, and the optimal distances and rates for intramolecular electron transfer, following the electron attachment into a specific Rydberg orbital [21–23].

In most discussions of ECD/ETD mechanisms, the ion/electron and ion/ion approaches are deemed to hold much in common, at least from the standpoint of the dynamics that occur once the electron is deposited into the ion. From the standpoint of the resulting dissociation, both methods appear to yield comparable results. For example, both give rise to cleavages at N–Cα bonds of peptide cations, both preserve labile PTMs, and both exhibit a propensity toward cleavage of disulfide linkages. There are, however, both fundamental differences between the approaches as well as differences in how the experiments are commonly implemented. For example, electron capture is inherently a more energetic process than electron transfer because the latter process requires that the electron affinity of the reagent species be overcome in order to transfer the electron. Most electron transfer reagents have electron affinities of 0.4–1.0 eV. There may also be differences in the initial population of electronic states in the radical cation species [23]. Evidence for peptide ion dipole effects that lead to differences between ECD and ETD behavior have been presented [24]. Another significant difference is that unlike the case for the ion/electron process, proton transfer always competes with electron transfer in the ion/ion process involving a multiply protonated analyte. In fact, most singly [25–27] and multiply charged [28–32] reagent anions used to date for ion/ion reactions remove protons from multiply protonated biomolecules and show essentially no propensity for electron transfer. Only a limited number of reagents have shown electron transfer to be competitive with proton transfer, which has been rationalized using a model based on Landau-Zener theory [33, 34]. Briefly, in order for electron transfer to compete with proton transfer, the reagent should have a low electron affinity (e.g., <2.0 eV) and favorable Franck-Condon factors for vertical electron detachment [35, 36].

Complicating factors in making careful comparisons of ETD and ECD data arise from differences in how ETD and ECD experiments are generally implemented. ETD is usually implemented in electrodynamic ion traps with bath gas pressures of 1–10 mTorr, whereas ECD is usually implemented in ion cyclotron resonance cells at background pressures of 10^{-8} Torr or lower. However, there are a few examples in which ECD has been implemented in ion traps with oscillating quadrupolar electric fields using relatively high bath gas pressures [37–40]. Such instruments employ reaction conditions much closer to those used for ETD. In this work, we have performed all experiments via ETD and via ECD in ion traps operated in the presence of a bath gas in the 1–10 mTorr pressure range to facilitate comparisons between ETD and ECD without the complication of the use of different pressure regimes.

This work follows a series of studies focused on the factors that affect ETD and extends the work, in this case, to ECD as well. This approach involves the systematic measurement of product partitioning of ion/ion and ion/electron reactions of model polypeptide ions. For example, it has been previously used to study how various characteristics of the reagent anion affect the ETD process [36], with particular emphasis placed on the competition between electron transfer and proton transfer, the role of the charge site within a given charge state [41] (similar studies have been conducted for ECD [42, 43]), the possible role of the amide hydrogen in the mechanism of ETD [44], and the role of cation charge state [45]. The latter studies augmented prior observations regarding the role of peptide charge state in ETD [46, 47]. In this work, emphasis was placed on the variation of cation

recombination energy (or, equivalently, charge per residue) in the absence of any change in net cation charge via variation of peptide size as well as the variation of reaction exothermicity via the identity of the 'reagent' (i.e., thermal electrons, radical anions of azobenzene and radical anions of 1,3-dinitrobenzene).

Experimental

Materials

The peptides XAGX, XAGAGX, and XAGAGAGAGX where both X's are either lysine (K), arginine (R), or histidine (H) residues, as well as peptides KAGKAGAGAG and KAGAG-KAGAG were custom synthesized by CPC Scientific (San Jose, CA, USA). Methanol and glacial acetic acid were purchased from Mallinckrodt (Phillipsburg, NJ, USA). Azobenzene and 1,3-dinitrobenzene were obtained from Sigma-Aldrich (St. Louis, MO, USA). Acetylation of the selected peptides was performed using a well-established protocol [48]. All peptide solutions were prepared to a concentration of about 50 μM for the ETD studies (10 μM for ECD experiments) in 49.5/49.5/1 (vol/vol/vol) mixture of methanol/water/acetic acid.

Mass Spectrometry

All electron transfer ion/ion reaction experiments were performed using a prototype version of a triple quadrupole/linear ion trap mass spectrometer (QTRAP; AB SCIEX, Concord, ON, Canada) [49]. A home-built dual ionization source equipped with a nanospray emitter for the formation of peptide cations and an atmospheric pressure chemical ionization (APCI) needle for the formation of the reagent radical anions was coupled directly to the interface of the QTRAP instrument. The procedure for the electron transfer ion/ion reactions has been described in detail elsewhere [50]. Briefly, independently mass-selected peptide cations and reagent radical anions were injected into the Q2 collision cell via Q1. Both ion polarities were stored in Q2 for various times and allowed to react in mutual storage mode [51, 52]. The electron transfer ion/ion reaction products were transferred from Q2 to Q3 for mass analysis via selective axial ejection (MSAE) [53]. The experiments were controlled using Daetalyst 3.14 research software provided by AB SCIEX. Azobenzene and 1,3-dinitrobenzene were chosen as reagents in this work because they have relatively high vapor pressures and readily form molecular anions under the APCI conditions used here. Reagents usually used in commercial systems such as fluoranthene [5] or azulene [54] undergo oxidation reactions upon ionization under the APCI conditions used here that lead to products that give rise to proton transfer.

The electron capture dissociation reactions were performed using a modified hybrid linear ion trap/time-of-flight (LIT/TOF nano-Frontier; Hitachi High Technologies, Tokyo, Japan) instrument [40]. Peptide cations were generated using a nanospray emitter while the electrons were created using a tungsten filament. The ions of interest were isolated in a linear quadrupole ion trap and transmitted to the ECD cell where the reaction took place. The peptide cations were allowed to react with the thermal electrons for 20 ms. The ion/electron reaction products were then released from the ECD cell and transmitted through an rf-only quadrupole and into the source region of the orthogonal acceleration/TOF for analysis. All of the ETD and ECD experiments were repeated at least three times.

Results and Discussion

The Roles of Cation Charge and Recombination Energy in Electron Transfer Probability

A number of factors go into in the curve-crossing model for rationalizing the probability for electron transfer. The model is described briefly here to provide context for the selection of

peptides and reagents used in this work. Electron transfer (ET) is assumed to occur at avoided crossings in the interaction between the reactant cation and anion. The cross section (σ_{ET}) for the two-body interaction is given by

$$\sigma_{ET} = P_{ET} \pi b_{ET}^2 \quad (1)$$

where P_{ET} is the probability of reaction at classical impact parameter b_{ET}.

The square of the impact parameter (in atomic units) takes the form [55]:

$$b_{ET}^2 = r_{ET}^2 \left[1 + \frac{2|Z_{cat} Z_{an}|}{r_{ET} \mu v_{rel}^2} \right] \quad (2)$$

where Z_{cat} and Z_{an} are the unit charges of the cationic and anionic reactants, respectively; v_{rel} is the relative velocity of the ions; μ is the reduced mass of the collision partners; and r_{ET} is the distance at which the electron transfer occurs. In this work, $Z_{cat}=2+$ and $Z_{an}=1-$ in all experiments. An estimate for r_{ET} can be taken as the distance at which the ground state curves of the entrance and exit channels cross, which, in atomic units, is given by:

$$r_{ET} \approx \frac{(Z_{cat} Z_{an})}{\Delta H_{ET}} \quad (3)$$

when at least one of the reactants is singly charged (as is the case here for the anionic reagent). The reaction enthalpy, ΔH_{ET}, is given by

$$\Delta H_{ET} = EA_R - RE_{cat} \quad (4)$$

where EA_R represents electron affinity of the reagent used to generate the anion and RE_{cat} represents the recombination energy of the cation.

The probability for electron transfer at the point at which the entrance and exit channels cross, P_{ET}, is modeled based on Landau-Zener theory [33, 34]. P_{ET} is determined by the non-adiabatic transition probability between states at the avoided crossing, P_{LZ}, by the relation:

$$P_{ET} = 2P_{LZ}(1 - P_{LZ}) \quad (5)$$

The expression for P_{LZ} is:

$$P_{LZ} = \exp \left(\frac{2\pi H_{12}^2 \langle \chi_{1v'} | \chi_{2v''} \rangle^2}{\frac{dr}{dt} \left(\frac{Z_{cat} Z_{an}}{r_{ET}^2} \right)} \right) \quad (6)$$

where H_{12} is the coupling matrix element at the point of closest approach, $< \chi_1 | \chi_2 >^2$ is the Franck-Condon (F-C) overlap between reactant and product vibrational wave functions associated with the transition from χ_1 to χ_2 for the reagent anion and its neutral counterpart, dr/dt is the radial velocity of the reactants at the crossing point and $Z_{cat}Z_{an}/r_{ET}^2$ gives the difference in the slopes of the entrance and exit channels at the crossing point. (The slope of the exit (product) channel is taken as zero because the charge of the reagent is zero in the product channel.) The radial velocity at the crossing point can be estimated by:

$$\frac{dr}{dt} \approx \left[\frac{2|Z_{cat}Z_{an}|}{r_{ET}\mu} \right]^{0.5} \quad (7)$$

The coupling matrix element, which indicates the strength of the electronic coupling between states, is extremely difficult to determine for the large polyatomic systems of relevance to this work. A parameterized expression for H_{12} described by Olson [56, 57], which is based on data collected for the reactions of a number of relatively small singly charged ions, has been used in our work. This expression allows for an estimation of the coupling matrix based upon EA_R and RE_{cat} values:

$$H_{12} = \left(1.044 \sqrt{EA_R} \sqrt{RE_{cat}} x \right) \cdot \exp(-0.875x) \quad (8)$$

$$where \quad x = \frac{r_{ETt}}{2} \left(\sqrt{2EA_R} + \sqrt{2RE_{cat}} \right). \quad (9)$$

Product Ion Partitioning

A major focus of this work is to follow the effect of changes in RE_{cat} on product partitioning in ETD and ECD. An important factor in determining RE_{cat} and, as a result, $H_{ET,}$ for a multiply charged ion is Z_{cat} [58]. It is clear from expressions (1)–(9), however, which Z_{cat} can affect $_{ET}$ in multiple ways. These include, for example, the roles that Z_{cat} plays in determining b_{ET}, r_{ET}, and dr/dt. For these reasons, the interpretation of the effect of changes in Z_{cat} in ETD is complicated by the various ways in which it affects $_{ET}$. To separate the role of RE_{cat} from the role of total charge in this work, we chose to examine model peptides ions in a single charge state (viz., doubly protonated peptides) of various size. To minimize site of protonation effects (e.g., arginine versus lysine versus histidine), peptides of the form XAGX, XAGAGX, and XAGAGAGAGX were compared with X = K, H, or R. RE_{cat} is expected to follow the order $[XAGX + 2H]^{2+} > [XAGAGX]^{2+} > [XAGAGAGAGX + 2H]^{2+}$ due to decreasing electrostatic repulsion and possible increasing charge solvation as the size of the polypeptide increases.

Figure 1 summarizes the product ion partitioning in ECD (Figure 1a) and in ETD (Figure 1b). In the case of ECD, electron capture is generally accepted as proceeding via initial capture into high lying Rydberg orbitals, as depicted by the electron orbit around a multiply protonated cation. The electron is presumed to evolve to lower lying Rydberg orbitals and eventually occupy the electronic states that give rise to ECD products. These states are represented in Figure 1a collectively as being present in the charge reduced intermediate. If the excited intermediate can be stabilized via emission or collision, a long-lived charge reduced species can be observed, which is represented by the EC,noD channel. Fragmentation channels are categorized as side-chain loss, backbone cleavage that gives rise to complementary c/z•-ions, and hydrogen atom loss (H•-loss). In the case of ETD, studies of the rates of reaction have suggested that the rate-determining step in gas-phase ion/ion reactions involving large polyatomic ions is the formation of a stable orbiting pair [59, 60], as depicted by the orbit in Figure 1b. This orbit can be considered to be the ion/ion analog to a high lying Rydberg state associated with ECD. Collapse of the orbit due to collisions and/ or tidal effects [61, 62] brings the reactants into close enough proximity for an electron to transfer from the anion to the cation or for a proton to transfer from the cation to the anion. At least some of the cation products from electron transfer will be generated in excited electronic states that can lead to dissociation. Stabilization of the intermediate via emission or collision can lead to the long-lived charge-reduced species, as represented by the ET,noD

channel. A complication in interpreting the product partitioning in ETD is the fact that proton transfer and electron transfer followed by H•-loss are indistinguishable. The ECD results proved to be particularly helpful in interpreting the ETD partitioning (vide infra).

Product partitioning is categorized here for ETD as proton transfer/H•-loss (PT/H•-loss), c/z•-ion formation (c/z•), side-chain loss (side chain), and electron transfer without dissociation (ET,noD). The analogous categories for ECD are H•-loss, c/z•-ion formation, side-chain loss, and electron capture without dissociation (EC,noD). Two levels of partitioning are reported. One emphasizes the partitioning between electron transfer/capture events that do not lead to a measurable change in analyte ion mass (i.e., the ET,noD and EC,noD channels) versus those that lead to a measurable change in analyte ion mass (i.e., the ECD, ETD, and PT channels). The other emphasizes partitioning among those specific channels that lead to a change in analyte ion mass (i.e., side-chain loss, c,z•-ion formation, and PT/H•-loss). For ETD, the partitioning definitions are:

$$\%ET, noD + \%ETD/PT/H \bullet -loss = 100\% \quad (10)$$

$$\%ETD/PT/H \bullet -loss = \frac{\sum(PT/H \bullet -loss + c/z \bullet + side - chain)}{\sum(PT/H \bullet -loss + c/z \bullet + side - chain + ET, noD)} \times 100 \quad (10.1)$$

$$\%ET, noD = \frac{\sum ET, noD}{\sum(PT/H \bullet -loss + c/z \bullet + side - chain + ET, noD)} \times 100 \quad (10.2)$$

and

$$\%PT/H \bullet -loss + c/z \bullet + side - chain = 100\% \quad (11)$$

$$\%PT/H \bullet -loss = \frac{\sum PT/H \bullet -loss}{\sum(PT/H \bullet -loss + c/z \bullet + side - chain)} \times 100 \quad (11.1)$$

$$\%c/z \bullet = \frac{\sum c/z \bullet}{\sum(PT/H \bullet -loss + c/z \bullet + side - chain)} \times 100 \quad (11.2)$$

$$\%side - chain = \frac{\sum side - chain}{\sum(PT/H \bullet -loss + c/z \bullet + side - chain)} \times 100. \quad (11.3)$$

The analogous relationships for ECD are:

$$\%EC, noD + \%ECD = 100\% \quad (12)$$

$$\%ECD = \frac{\sum(H \bullet -loss + c/z \bullet + side - chain)}{\sum(H \bullet -loss + c/z \bullet + side - chain + EC, noD)} \times 100 \quad (12.1)$$

$$\%EC, noD = \frac{\sum EC, noD}{\sum(H \bullet -loss + c/z \bullet + side - chain + EC, noD)} \times 100 \quad (12.2)$$

and

$$\%ECD + c/z\bullet + side-chain = 100\% \quad (13)$$

$$\%H\bullet -loss = \frac{\sum H\bullet -loss}{\sum(H\bullet -loss + c/z\bullet + side-chain)} \times 100 \quad (13.1)$$

$$\%c/z\bullet = \frac{\sum c/z\bullet}{\sum(H\bullet -loss + c/z\bullet + side-chain)} \times 100 \quad (13.2)$$

$$\%side-chain = \frac{\sum side-chain}{\sum(H\bullet -loss + c/z\bullet + side-chain)} \times 100. \quad (13.3)$$

The only difference between the two sets of relationships for ETD and ECD is the explicit recognition of the contribution from proton transfer in the former case, which cannot be distinguished from electron transfer followed by H•-loss.

Tables 1 and 2 list the product ion partitioning in the ETD of the doubly protonated $X(AG)_nX$ peptides using azobenzene (EA=0.6 eV) and 1,3-dinitrobenzene (EA=1.7 eV), respectively, and Table 3 summarizes the analogous results for ECD. In all three cases, doubly protonated peptides with n =1, 2, and 4 for X = K, R, and H were examined. To determine if the relative positions of the basic residues is a key factor in these experiments, the doubly protonated isomeric peptides KAGAGAGAGK, KAGAGKAGAG, and KAGKAGAGAGAG were subjected to both ETD and ECD. To determine the possible role of the N-terminus in the X = R and H peptides, the N-terminally acetylated doubly protonated Ac-RAGAGR and Ac-HAGAGH were subjected to ETD.

A number of observations can be drawn from examination of the results in Tables 1, 2, and 3. First, the results are fully consistent with prior observations that distinguished the ETD behaviors of the three common basic residues [41]. For example, the peptides with X = H showed the greatest contribution of ET,noD. The only model peptide dication to show significant EC,noD was HAGAGAGAGH. This observation is consistent with the 'histidine' effect described by Ture ek et al. [63–66], which arises from an isomerization process that takes place within the radical species generated by electron capture by the protonated imidazole side chain. The greatest degree of side-chain cleavage was noted for the X = R peptide cations, which may be related to the reportedly poor H•-donating capability of the hypervalent arginine side-chain radical [67]. The greatest relative contribution from cleavages to yield complementary c/z•-ions was noted for X = K. The experiments with N-terminally acetylated X = H and X = R peptides, which precluded any contributions that might arise due to proton solvation by a primary amine, lead to increased contributions from ET,noD and side-chain loss, respectively. The effect of acetylation was most significant for the X = H peptides, which showed the unmodified ion to yield 20 % ET,noD while the N-terminally acetylated version of the ion yielded 35 % ET,noD.

A second set of observations addressed the importance of the relative positions of the basic residues versus peptide size. The issue revolves around whether the isomeric KAGAGAGAGK, KAGAGKAGAG, and KAGKAGAGA-GAG ions would show product partitioning similar to one another, product partitioning similar to the smaller peptides with the same number of AG residues between lysines (e.g., KAGKAGAGAG versus KAGK), or some intermediate partitioning. At the level of partitioning provided in Tables 1, 2, and 3,

the three isomeric 10-mer polypeptide ions behaved much more similarly to one another than to any of the smaller peptides for each of the respective experiments (i.e., ETD with azobenzene, ETD with 1,3-dinitro-benzene, and ECD). While the three isomeric peptide ions showed quite similar overall partitioning into $c/z\bullet$ ions with a given "reagent" (viz., anion or electron), they each showed somewhat different partitioning among the various individual $c/z\bullet$ channels (see Figure 4, which is discussed further below). The relative abundances of $c/z\bullet$ is a subject of current study within the ECD/ETD community [68–71] but is not a primary focus of this work. For example, the ECD experiment for doubly protonated KAGKAGAGAG yielded a small relative proportion of H•-loss, a 3 %–4 % value similar to the other isomeric 10-mer cations, while the KAGK cation shows H•-loss to be roughly 36 % of the total ECD products. This set of observations clearly shows that the peptide size for a given charge (or, equivalently, charge per residue) is more important in determining product partitioning than is the relative location of the basic residues in the peptide sequence. See also a recent report that relates peptide size-dependent ECD behavior for a range of tryptic peptides [72].

A third set of observations indicates that for all direct comparisons in the ETD experiments summarized in Tables 1 and 2, the %PT/H•-loss channel was significantly lower for azobenzene than for 1,3-dinitrobenzene. For example, a range of 17 %–21 % for the %PT/H•-loss channel was noted for the three isomeric 10-mer cations in reactions with the azobenzene radical anion whereas a range of 76 %–79 % for the %PT/H•-loss channel was observed in reactions with the dinitrobenzene anion. Given that there is uncertainty in the last significant digit in these measurements, the %PT/H•-loss values for the three isomeric cations with a given reagent anion are within experimental error whereas the values for the two different reagents are quite different. This observation is consistent with previous studies on the role of the reagent anion in the competition between electron transfer and proton transfer [36]. A change in the electron affinity of the reagent in the model summarized above has a major impact in determining the probability for electron transfer, P_{ET}, via its role in determining H_{ET}, r_{ET}, and H_{12}. The F-C factors associated with each reagent also affect H_{12}. Figure 2 compares plots of P_{ET} for azobenzene and 1,3-dinitrobenzene as a function of cation RE using the model summarized, the Olson parameterization for H_{12}, and assuming EA=0.6 eV, F-C=0.18 for azobenzene and EA=1.7 eV, F-C=0.27 for 1,3-dinitrobenzene. Also indicated in the figure is the range of cation recombination energies likely to be relevant to this study.

Given the assumptions and uncertainties in the values used in the model, the positions of the curves are expected to be semiquantitative at best. However, they are useful in making qualitative comparisons of different reagents. The curves in Figure 2 represent those for the generation of products in ground electronic states and therefore suggest that there is an optimal cation recombination energy. However, the cations are generally believed to be formed in excited electron states, the curves for which are shifted to the right of the respective ground state curves. The significance of crossings that lead to the population of excited electronics states in the context of Figure 2 is that the decrease in P_{ET} at high RE values may not be observed as the probabilities for crossings into excited electronic states are expected to be increasingly likely as RE increases. However, if the cation RE is on the low side of the maximum, there are no lower energy states to populate. Hence, while the cation RE may not become too high to observe electron transfer, it can be too low. Figure 2 is consistent with the greater extent of electron transfer with the azobenzene anions than with 1,3-dinitrobenzene anions provided the cation recombination energies are not all fully to the right of the 1,3-dinitrobenzene curve.

While the comparison of Tables 1 and 2 is consistent with previous findings regarding the relative efficiencies of azobenzene and dinitrobenzene anions as ETD reagents, the fact that

proton transfer on one hand, and electron transfer followed by H•-loss on the other, give the same products introduces some ambiguity in interpretation. For example, a curious trend in %PT/H•-loss is noted for the K(AG)$_n$K ions for both reagents. The %PT/H•-loss observed with azobenzene anions was 26 % for doubly protonated KAGK, 10 % for doubly protonated KAGAGK, and 17 %–21 % for the isomeric 10-mer dications. The analogous %PT/H•-loss values for the dinitrobenzene anions were 64 % for KAGK, 43 % for KAGAGK, and 76 %–79 % for the three isomeric 10-mer dications. The fact that the %PT/H•-loss values for the KAGK dications are higher than those for the KAGAGK ions with both reagent anions is inconsistent with the expected trend in RE values for the respective doubly protonated peptides (i.e., KAGK>KAGAGK>KAGAGAGAGK) if proton transfer is the dominant process. Higher cation RE values are expected to increase the probability for electron transfer (see Figure 2). This observation, however, may not be inconsistent with expectation if electron transfer followed by H•-loss is relatively more important for the smaller peptide than for the larger peptides. The ECD data of Table 3 are particularly informative in this regard. The contribution of the H•-loss channel is clearly inversely related to charge per residue in the ECD data. This observation suggests that the relatively high %PT/H•-loss values for the KAGK dications arises from higher relative contributions from H•-loss than occurs with the larger dications. We speculate that the reason for greater H•-loss from high charge per residue peptides may be due to a structural effect from high electrostatic repulsion. Solvation of excess charge via interaction with polar groups, such as the carbonyl oxygens of the backbone, may be minimized when the excess charges are in close proximity. Such an intramolecular solvation interaction facilitates H•-transfer to an amide linkage and is a key element in the so-called 'Cornell' mechanism for ECD to produce complementary c/z•-ions [12]. In the absence of a preexisting interaction between the excess charge and the peptide backbone, the likelihood for capture/transfer of the hydrogen radical is diminished, thereby giving rise to greater H•-loss.

It is noteworthy that the relative contribution from H•-loss in the ECD of the doubly protonated XAGX ions exceeds significantly the combined PT/H•-loss contribution for the same ions from reaction with azobenzene anions (compare Tables 1 and 3). This indicates that H•-loss takes place more readily from the ions of highest charge per residue under ECD conditions than under ETD conditions, at least for the azobenzene anions. The underlying reason why H•-loss might be more likely under ECD conditions than ETD conditions for the high charge per residue ions is not readily apparent from these data. Several differences between the electron capture and electron transfer processes might play a role. For example, electron capture is always a more exothermic process than electron transfer as the electron affinity of the reagent must be overcome in the latter process. The relevant studies to date suggest that H•-loss is increasingly competitive at higher internal energies [73]. If it is assumed that both ECD and ETD proceed through an evolution in electronic states from the initially formed Rydberg states to lower-lying states (i.e., a process of intramolecular electron transfer), and that H•-loss, c/z•-ion formation, and side-chain loss can take place via different electronic states, the initial population of electronic states might be important in determining product ion partitioning. Differences in initial excited electronic state population in electron capture versus electron transfer might therefore play a role in differences in product ion partitioning between ECD and ETD [23, 74].

While differences in total internal energy between ECD and ETD, which may also be reflected in different partitioning in excited electronic states, may account for different extents of H•-loss, an alternative factor for the lesser extent of H•-loss from high charge per residue peptides in ETD versus ECD is differences in the angular momenta, J, of the incipient charge-reduced peptides (i.e., [X(AG)$_n$X+2H]$^{+•}$) produced via an ion/ion versus an ion/electron process, as indicated in reaction (14):

$$[X(AG)_n X+2H]^{2+}+A^{-\bullet}(or\ e^-) \rightarrow [X(AG)_n X+2H]^{+\bullet} \rightarrow products \quad (14)$$
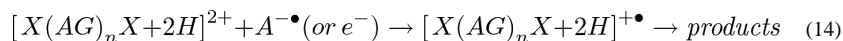
The angular momentum, L, associated with a two-body interaction is given by:

$$L=\mu v_{rel} b \quad (15)$$

where μ is the reduced mass of the collision partners, b is the impact parameter, and v_{rel} is the initial relative velocity of the collision partners. It is apparent from relation (15) that angular momentum effects are most likely to be observed with large impact parameter processes. At comparable impact parameters, however, the low mass of the electron leads to values of L for the ion/electron case that are orders of magnitude lower than those for the ion/ion case. The importance of angular momentum in dissociation, particularly for H•-loss, has already been discussed for ion/molecule reactions [75–78], which have substantially smaller impact parameters than ion/ion reactions. Long-lived intermediates generated by reactions of ions with molecules can be formed in which all of the initial angular momentum of the pair, L, is converted to angular momentum of the collision complex, J. The magnitude of J is significant for subsequent dissociation of the complex as the rotation of the collision complex creates rotational barrier in the exit channel. The magnitude of the rotational barrier, $V_{eff,rot}$, to a first approximation, is given by [75]:

$$V_{eff,rol}=\frac{J^4}{8\alpha e^2 \mu^2} \quad (16)$$

where   is the polarizability of the neutral and μ, in this case, is the reduced mass of the dissociation products. Of all of the ETD/ECD dissociation channels, the rotational barrier for the reaction:

$$[X(AG)_n X+2H]^{+\bullet} \rightarrow [X(AG)_n X+2H]^{+}+H\bullet \quad (17)$$
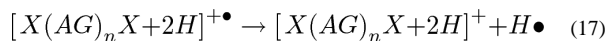
is highest due to the low polarizability of the hydrogen atom (0.667 Å^3)[75] and the fact that the products have the lowest reduced mass of all of the possible dissociation channels. For these reasons, a higher degree of angular momentum in the incipient charge-reduced product formed via ETD versus ECD is deemed to be the most likely interpretation for why ECD leads to a higher degree of H•-loss for the high charge per residue peptides. This conclusion is tempered by a lack of detailed understanding of the dynamics of the ion/ion reaction that might otherwise allow for an estimation of the L   J efficiency (i.e., the extent to which the angular momentum of the orbiting pair is partitioned into rotation of the charge reduced peptide versus the other available channels, such as the relative translation of the charge-reduced peptide and the neutralized reagent, rotation of the reagent, etc.).

c/z•-Ion Channels in ETD/ECD

Tables 1, 2, and 3 provide partitioning into the main categories of ECD/ETD dissociation channels (viz., H•-loss, side-chain loss, and c/z•-formation). It is also of interest to compare ECD and ETD for partitioning among these categories, particularly for the sequence informative channels that lead to c/z•-ions. Figures 3 and 4 compare the relative contributions of the various dissociation channels that lead to c/z•-ions from ECD and ETD (azobenzene reagent) for the various lysine-containing model peptides. Contributions from side-chain loss are also included for both cases and H•-loss is included in the ECD data. Comparison of the ECD and ETD data for KAGK (Figure 3a and c, respectively), for example, shows preference for the same backbone cleavages; the c_3-ion is dominant in both ECD and ETD. The extent of side chain loss is also very similar in both cases. Doubly

protonated KAGAGK behaves in a similar manner as demonstrated in Figure 3b and d where the c_3 channel is again the most dominant. The pattern of abundances of the c_n ions is also similar.

In fact, the patterns of c/z•-ions in the ECD and ETD spectra were similar for all of the lysine-containing peptides. Figure 4 compares the results for the ECD and ETD (azobenzene as reagent) for the isomeric lysine-containing 10-mers. The similarities in the fragmentation patterns are remarkable considering that the spectra were collected using different instrument platforms (viz., hybrid triple quadrupole/linear-ion-trap versus linear ion trap/ time-of-flight). The ETD experiments generally yielded lower relative abundances for the products of low mass/charge than did the ECD experiments (compare, for example, the spectra of Figures 4a and d), which may reflect differences in collection/detection efficiencies in the two instruments. The pattern of c/z•-ions (i.e., the identities and abundances of the c/z•-ions relative to one another) was also remarkably similar in the ETD spectra generated with 1,3-dinitrobenzene anions (data not shown).

A summary of the dissociation product partitioning for the arginine and histidine-containing model peptides is provided in Figures 5 and 6, respectively. In the case of the $R(AG)_nR$ peptides, the c/z•-ion patterns again appear to be similar for the n=1 and n=2 peptides, recognizing the apparent lower relative collection/detection efficiencies for the ETD experiment. The ETD experiment yielded significantly fewer c/z•-ions, both in variety and relative abundance, than did the ECD experiment for the $R(AG)_4R$ dication, however. The %c/z for this ion was the lowest of all the model peptides for both ETD reagents while the PT/H•-loss and side-chain loss channels were both relatively high. Furthermore, most of the c/z•-ion product signal was concentrated in the c_9-ion.

In the case of the $H(AG)_nH$ peptide dications (see Figure 6), the ECD and ETD c/z•-ion patterns were quite similar for the $H(AG)_4H$ ion, whereas ECD yielded a somewhat lower variety of c/z•-ions than did ETD for the smaller peptide ions. This observation may well be related to the fact that the small histidine-containing ions yielded the highest contributions from H•-loss under ECD conditions. If the angular momentum argument described above is a significant factor, an increased barrier for H•-loss in the charge-reduced peptide ions generated via ETD may allow more H•-transfer channels that lead to c/z•-ions to compete with H•-loss.

Conclusions

A series of doubly protonated model peptides of the form $X(AG)_nX$ have been subjected to ECD and ETD in electrodyamic ion traps operated in the presence of a bath gas in the milliTorr pressure regime. A full accounting of the various competitive product ion channels was performed as a function of several experimental variables. These included the identity of the basic amino acids present in the peptide (X = K, R, or H), the length of the peptide (n=1, 2, or 4), and the reagent (near-thermal electrons, anions of azobenzene, or anions of 1.3-dinitrobenzene). By varying n, for a given charge state, it is possible to follow effects due to changes in recombination energy (or charge per residue). By varying X, it is possible to follow effects due to sites of protonation. By varying reagents, it is possible to follow effects due to changes in reagent electron affinity and reagent mass.

The results obtained in this work with both ECD and ETD are fully consistent with previous studies on the role of protonation site on product ion partitioning in ETD. The fact that proton transfer and electron transfer followed by H•-loss both lead to the same nominal product in ETD, complicates interpretation of product channel partitioning in ETD studies. The ECD results were instructive in this regard in that they showed the tendency for H•-loss

to correlate with charge per residue. Proton transfer, on the other hand, is expected to be inversely related to charge per residue (i.e., recombination energy). In general, the observed trends in %PT/H•-loss were consistent with expectation for $n=1$, 2, and 4 and for the two anionic reagents. The apparently anomalous ETD behavior of the $K(AG)_nK$ peptides, which showed relatively high %PT/H•-loss values for the smallest peptides, can be rationalized by relatively high contributions from electron transfer followed by H•-loss, as suggested by the ECD data. Interestingly, ECD appears to lead to higher degrees of H•-loss from ions of high charge per residue than does ETD. This observation may arise from differences in internal energies, which would be reflected in different initial population of different electronic excited states. An alternative possible factor introduced here is differences in the angular momenta of the charge-reduced peptide ions generated by electron capture (low additional angular momentum) versus electron transfer (high additional angular momentum). The angular momentum effect may also enhance the likelihood for ET,noD relative to EC,noD, although the data set generated here is likely to be too small to draw a general conclusion. Finally, the partitioning among the various c/z•-ion channels was remarkably similar in ECD and ETD for most of the model peptides studied despite the differences in the electron capture and electron transfer processes.

Acknowledgments

References

1. McLuckey SA, Mentinova M. Ion/neutral, ion/electron, ion/photon, and ion/ion interactions in tandem mass spectrometry: Do we need them all? Are they enough? J Am Soc Mass Spectrom. 2011; 22:3–12. [PubMed: 21472539]

2. Wells JM, McLuckey SA. Collision-induced dissociation (CID) of peptides and proteins. Methods Enzymol. 2005; 402:148–185. [PubMed: 16401509]

3. Little DP, Speir JP, Senko MW, O'Connor PB, McLafferty FW. Infrared multiphoton dissociation of large multiply-charged ions for biomolecule sequencing. Anal Chem. 1994; 66:2809–2815. [PubMed: 7526742]

4. Zubarev RA, Kelleher NL, McLafferty FW. Electron capture dissociation of multiply charged protein cations. A nonergodic process. J Am Chem Soc. 1998; 120:3265–3266.

5. Syka JE, Coon JJ, Schroeder MJ, Shabanowitz J, Hunt DF. Peptide and protein sequence analysis by electron transfer dissociation mass spectrometry. Proc Natl Acad Sci USA. 2004; 101:9528–9533. [PubMed: 15210983]

6. Coon JJ. Collisions or electrons? Protein sequence analysis in the 21st century. Anal Chem. 2009; 81:3208–3215. [PubMed: 19364119]

7. Coon JJ, Syka JEP, Shabanowitz J, Hunt DF. Anion dependence in the partitioning between proton and electron transfer in ion/ion reactions. Int J Mass Spectrom. 2004; 236:33–42.

8. Pitteri SJ, Chrisman PA, McLuckey SA. Electron-transfer ion/ion reactions of doubly protonated peptides: Effect of elevated bath gas temperature. Anal Chem. 2005; 77:5662–5669. [PubMed: 16131079]

9. Gunawardena HP, Gorenstein L, Erickson DE, Xia Y, McLuckey SA. Transmission mode ion/ion electron-transfer dissociation in a linear ion trap. Int J Mass Spectrom. 2007; 265:130–138.

10. Breuker K, Oh H, Lin C, Carpenter BK, McLafferty FW. Nonergodic and conformational control of the electron capture dissociation of protein cations. Proc Natl Acad Sci USA. 2004; 101:14011–14016. [PubMed: 15381764]

11. Ture ek F. N–C bond dissociation energies and kinetics in amide and peptide radicals. Is the dissociation a non-ergodic process? J Am Chem Soc. 2003; 125:5954–5963. [PubMed: 12733936]

12. Zubarev RA, Kruger NA, Fridriksson EK, Lewis MA, Horn DM, Carpenter BK, McLafferty FW. Electron capture dissociation of gaseous multiply-charged proteins is favored at disulfide bonds and other sites of high hydrogen atom affinity. J Am Chem Soc. 1999; 121:2857–2866.

13. Zubarev RA. Reactions of polypeptide ions with electrons in the gas phase. Mass Spectrom Rev. 2003; 22:57–77. [PubMed: 12768604]

14. Zubarev RA, Haselmann KF, Budnik B, Kjeldsen F, Jensen F. Towards an understanding of the mechanism of electron-capture dissociation: A historical perspective and modern ideas. Eur J Mass Spectrom. 2002; 8:337–349.

15. Hudgins, R.; Hakansson, K.; Quinn, JP.; Hendrickson, CL.; Marshall, AG. Proceedings of the 50th ASMS Conference on Mass Spectrometry and Allied Topics; Orlando, Florida. June 2–6, 2002; p. A020420

16. Syrstad EA, Ture ek F. Toward a general mechanism of electron capture dissociation. J Am Soc Mass Spectrom. 2005; 16:208–224. [PubMed: 15694771]

17. Sobczyk M, Anusiewicz W, Berdys-Kochanska J, Sawicka A, Skurski P, Simons J. Coulomb-assisted dissociative electron attachment: Application to a model peptide. J Phys Chem A. 2005; 109:250–258. [PubMed: 16839114]

18. Anusiewicz W, Berdys-Kochanska J, Simons J. Electron attachment step in electron capture dissociation (ECD) and electron transfer dissociation (ETD). J Phys Chem A. 2005; 109:5801–5813. [PubMed: 16833914]

19. Anusiewicz W, Berdys-Kochanska J, Skurski P, Simons J. Simulating electron transfer attachment to a positively charged model peptide. J Phys Chem A. 2006; 110:1261–1266. [PubMed: 16435786]

20. Sobczyk M, Simons J. The role of excited Rydberg states in electron transfer dissociation. J Phys Chem B. 2006; 110:7519–7527. [PubMed: 16599533]

21. Neff D, Simons J. Analytical and computational studies of intramolecular electron transfer pertinent to electron transfer and electron capture dissociation mass spectrometry. J Phys Chem A. 2010; 114:1309–1323. [PubMed: 19731901]

22. Simons J. Mechanisms for S–S and N–C bond cleavage in peptide ECD and ETD mass spectrometry. Chem Phys Lett. 2010; 484:81–95.

23. Simons J. Analytical model for rates of electron attachment and intramolecular electron transfer in electron transfer dissociation mass spectrometry. J Am Chem Soc. 2010; 132:7074–7085. [PubMed: 20438123]

24. Moss CL, Chung TW, Wyer JA, Nielsen SB, Hvelplund P, Ture ek F. Dipole-guided electron capture causes abnormal dissociations of phosphorylated pentapeptides. J Am Soc Mass Spectrom. 2011; 22:731–751. [PubMed: 21472611]

25. Loo RRO, Udseth HR, Smith RD. Evidence of charge inversion in the reaction of singly charged anions with multiply charged macroions. J Phys Chem. 1991; 95:6412–6415.

26. Stephenson JL, McLuckey SA. Ion/ion reactions in the gas phase: Proton transfer reactions involving multiply-charged proteins. J Am Chem Soc. 1996; 118:7390–7397.

27. Scalf M, Westphall MS, Krause J, Kaufman SL, Smith LM. Controlling charge states of large ions. Science. 1999; 283:194–197. [PubMed: 9880246]

28. Loo RRO, Udseth HR, Smith RD. A new approach for the study of gas-phase ion-ion reactions using electrospray ionization. J Am Soc Mass Spectrom. 1992; 3:695–705.

29. Wells JM, Chrisman PA, McLuckey SA. "Dueling" ESI: Instrumentation to study ion/ion reactions of electrospray-generated cations and anions. J Am Soc Mass Spectrom. 2002; 13:614–622. [PubMed: 12056562]

30. Wells JM, Chrisman PA, McLuckey SA. Formation of protein–protein complexes in vacuo. J Am Chem Soc. 2001; 123:12428–12429. [PubMed: 11734052]

31. He M, McLuckey SA. Two ion/ion charge inversion steps to form a doubly protonated peptide from a singly protonated peptide in the gas phase. J Am Chem Soc. 2003; 125:7756–7757. [PubMed: 12822966]

32. He M, Emory JE, McLuckey SA. Reagent anions for charge inversion of polypeptide/protein cations in the gas phase. Anal Chem. 2005; 77:3173–3182. [PubMed: 15889906]

33. Landau LD. Zur Theorie der Energieubertragung. II. Phys Z. 1932; 2:46–51.

34. Zener C. Non-adiabatic crossing of energy levels. Proc R Soc Lond A. 1932; 137:696–702.

35. McLuckey SA. The emerging role of ion/ion reactions in biological mass spectrometry: Considerations for reagent ion selection. Eur J Mass Spectrom. 2010; 16:429–439.

36. Gunawardena HP, He M, Chrisman PA, Pitteri SJ, Hogan JM, Hodges BDM, McLuckey SA. Electron transfer versus proton transfer in gas-phase ion/ion reactions of polyprotonated peptides. J Am Chem Soc. 2005; 127:12627–12639. [PubMed: 16144411]

37. Baba T, Hashimoto Y, Hasegawa H, Hirabayashi A, Waki I. Electron capture dissociation in a radio frequency ion trap. Anal Chem. 2004; 76:4263–4266. [PubMed: 15283558]

38. Silivra OA, Kjeldsen F, Ivonin IA, Zubarev RA. Electron capture dissociation of polypeptides in a three-dimensional quadrupole ion trap: Implementation and first results. J Am Soc Mass Spectrom. 2005; 16:22–27. [PubMed: 15653360]

39. Ling L, Brancia FL. Electron capture dissociation in a digital ion trap mass spectrometer. Anal Chem. 2006; 78:1995–2000. [PubMed: 16536438]

40. Satake H, Hasegawa H, Hirabayashi A, Hashimoto Y, Baba T, Masuda K. Fast multiple electron capture dissociation in a linear radio frequency quadrupole ion trap. Anal Chem. 2007; 79:8755–8761. [PubMed: 17902701]

41. Xia Y, Gunawardena HP, Erickson DE, McLuckey SA. Effects of cation charge-site identity and position on electron-transfer dissociation of polypeptide cations. J Am Chem Soc. 2007; 129:12232–12243. [PubMed: 17880074]

42. Ivarone AT, Peach K, Williams ER. Effects of charge state and cationizing agent on the electron capture dissociation of a peptide. Anal Chem. 2004; 76:2231–2238. [PubMed: 15080732]

43. Tsybin YO, Haselmann KF, Emmett MR, Hendrickson CL, Marshall AG. Charge location directs electron capture dissociation of peptide dications. J Am Soc Mass Spectrom. 2006; 17:1704–1711. [PubMed: 16963276]

44. Crizer DM, McLuckey SA. Electron transfer dissociation of amide nitrogen methylated polypeptide cations. J Am Soc Mass Spectrom. 2009; 20:1349–1354. [PubMed: 19410483]

45. Liu J, McLuckey SA. Electron transfer dissociation: Effects of cation charge state on product partitioning in ion/ion electron transfer to multiply protonated polypeptides. Int J Mass Spectrom. 2012; 330/332:174–181. [PubMed: 23264749]

46. Good DM, Wirtala M, McAlister GC, Coon JJ. Performance characteristics of electron transfer dissociation mass spectrometry. Mol Cell Proteom. 2007; 6:1942–1951.

47. Pitteri SJ, Chrisman PA, Hogan JM, McLuckey SA. Electron transfer ion/ion reactions in a three-dimensional quadrupole ion trap: Reactions of doubly and triply protonated peptides with $SO_2^{-\bullet}$. Anal Chem. 2005; 77:1831–1839. [PubMed: 15762593]

48. Reid GE, Simpson RJ, O'Hair RAJ. A mass spectrometric and ab initio study of the pathways for dehydration of simple glycine and cysteine-containing peptide $[M + H]^+$ ions. J Am Soc Mass Spectrom. 1998; 9:945–956.

49. Hager JW. A new linear ion trap mass spectrometer. Rapid Commun Mass Spectrom. 2002; 16:512–526.

50. Liang X, Xia Y, McLuckey SA. Alternately pulsed nanoelectrospray ionization/atmospheric pressure chemical ionization for ion/ion reactions in an electrodynamic ion trap. Anal Chem. 2006; 78:3208–3212. [PubMed: 16643016]

51. Xia Y, Wu J, Londry FA, Hager JW, McLuckey SA. Mutual storage mode ion/ion reactions in a hybrid linear ion trap. J Am Soc Mass Spectrom. 2005; 16:71–81. [PubMed: 15653365]

52. Xia Y, Liang X, McLuckey SA. Pulsed dual electrospray ionization for ion/ion reactions. J Am Soc Mass Spectrom. 2005; 16:1750–1756. [PubMed: 16182558]

53. Londry FA, Hager JW. Mass selective axial ion ejection from a linear quadrupole ion trap. J Am Soc Mass Spectrom. 2003; 14:1130–1147. [PubMed: 14530094]

54. Compton PD, Strukl JV, Bai DL, Shabanowitz J, Hunt DF. Optimization of electron transfer dissociation via informed selection of reagents and operating parameters. Anal Chem. 2012; 84:1781–1785. [PubMed: 22182179]

55. Mahan BH. Recombination of gaseous ions. Adv Chem Phys. 1973; 23:1–40.

56. Olson RE. Absorbing-sphere model for calculating ion-ion recombination total cross sections. J Chem Phys. 1972; 56:2979–2991.

57. Olson RE, Smith FT, Bauer E. Estimation of the coupling matrix elements for one-electron transfer systems. Appl Opt. 1971; 10:1848–1855. [PubMed: 20111217]

58. Budnik BA, Tsybin YO, Hakansson P, Zubarev RA. Ionization energies of multiply protonated polypeptides obtained by tandem ionization in Fourier transform mass spectrometers. J Mass Spectrom. 2002; 37:1141–1144. [PubMed: 12447890]

59. Stephenson JL Jr, McLuckey SA. Ion/ion reactions in the gas-phase: Proton transfer reactions involving multiply-charged proteins. J Am Chem Soc. 1996; 118:7390–7397.

60. Wells JM, Chrisman PA, McLuckey SA. Formation and characterization of protein–protein complexes in vacuo. J Am Chem Soc. 2003; 125:7238–7249. [PubMed: 12797797]

61. Bates DR, Morgan WL. New recombination mechanism -tidal termolecular ionic recombination. Phys Rev Lett. 1990; 64:2258–2260. [PubMed: 10041628]

62. Morgan WL, Bates DR. Tidal termolecular ionic recombination. J Phys B At Mol Opt Phys. 1992; 25:5421–5430.

63. Ture ek F, Jones JW, Towle T, Panja S, Nielsen SB, Hvelplund P, Paizs B. Hidden histidine radical rearrangements upon electron transfer to gas-phase peptide ions. Experimental evidence and theoretical analysis. J Am Chem Soc. 2008; 130:14584–14596. [PubMed: 18847261]

64. Ture ek F, Chen XH, Hao CT. Where does the electron go? Electron distribution and reactivity of peptide cation radicals formed by electron transfer in the gas phase. J Am Chem Soc. 2008; 10:8818–8833. [PubMed: 18597436]

65. Chung TW, Ture ek F. Amplified histidine effect in electron transfer dissociation of histidine rich peptides from histatin 5. Int J Mass Spectrom. 2011; 306:99–107.

66. Ture ek F, Chung TW, Moss CL, Wyer JA, Ehlerding A, Holm AIS, Zettergren H, Nielsen SB, Hvelplund P, Rooke JC, Bythell B, Paizs B. The histidine effect. Electron transfer and capture cause different dissociations and rearrangements of histidine peptide cation-radicals. J Am Chem Soc. 2010; 132:10728–10740. [PubMed: 20681705]

67. Chen X, Ture ek F. The arginine anomaly: Arginine radicals are poor hydrogen atom donors in electron transfer induced dissociations. J Am Chem Soc. 2006; 128:12520–12530. [PubMed: 16984203]

68. Tsybin YO, Haselmann KF, Emmett MR, Hendrickson CL, Marshall AG. Charge location directs electron capture dissociation. J Am Soc Mass Spectrom. 2006; 17:1704–1711. [PubMed: 16963276]

69. Vorobyev A, Ben Hamidane H, Tsybin YO. Electron capture dissociation product ion abundances at the X amino acid in RAAAA-X-AAAAK peptides correlate with amino acid polarity and radical stability. J Am Soc Mass Spectrom. 2003; 20:2273–2283. [PubMed: 19811930]

70. Simons J, Ledvina AR. Spatial extent of fragment-ion abundances in electron transfer dissociation and electron capture dissociation mass spectrometry of peptides. Int J Mass Spectrom. 2012; 330:84–94.

71. Ture ek F, Moss CL, Chung TW. Correlating ETD fragment ion intensities with peptide ion conformational and electronic structure. Int J Mass Spectrom. 2012; 330:207–219.

72. van der Rest G, Hui R, Frison G, Chamot-Rooke J. Dissociation channel dependence on peptide size observed in electron capture dissociation of tryptic peptides. J Am Soc Mass Spectrom. 2011; 22:1631–1644. [PubMed: 21953266]

73. Syrstad EA, Stephens DD, Ture ek F. Hydrogen atom adducts to the amide bond. Generation and energetics of amide radicals in the gas phase. J Phys Chem A. 2003; 107:115–126.

74. Moss CL, Liang W, Li X, Ture ek F. The early life of a peptide cation-radical. Ground and excited-state trajectories of electron-based peptide dissociations during the first 330 femtoseconds. J Am Soc Mass Spectrom. 2012; 23:446–459. [PubMed: 22187160]

75. Meisels GG, Verboom GML, Weiss MJ, Hsieh T. Angular momentum in ion-molecule reactions. J Am Chem Soc. 1979; 101:7189–7195.

76. Chesnavich WJ, Bowers MT. Statistical phase space theory of polyatomic systems. Application to the cross section and product kinetic energy distribution of the reaction $C_2H_4^{+\bullet} + C_2H_4 \quad C_3H_5+ + CH_3^{\bullet}$. J Am Chem Soc. 1976; 98:8301–8309.

77. Chesnavich WJ, Bowers MT. Statistical phase space theory of polyatomic systems: Rigorous energy and angular momentum conservation in reactions involving symmetric polyatomic species. J Chem Phys. 1977; 66:2306–2315.

78. Verboom GML, Meisels GG. Angular momentum distributions in collision processes and the location of the transition state in ion-molecule reactions. J Chem Phys. 1978; 68:2714–2717.
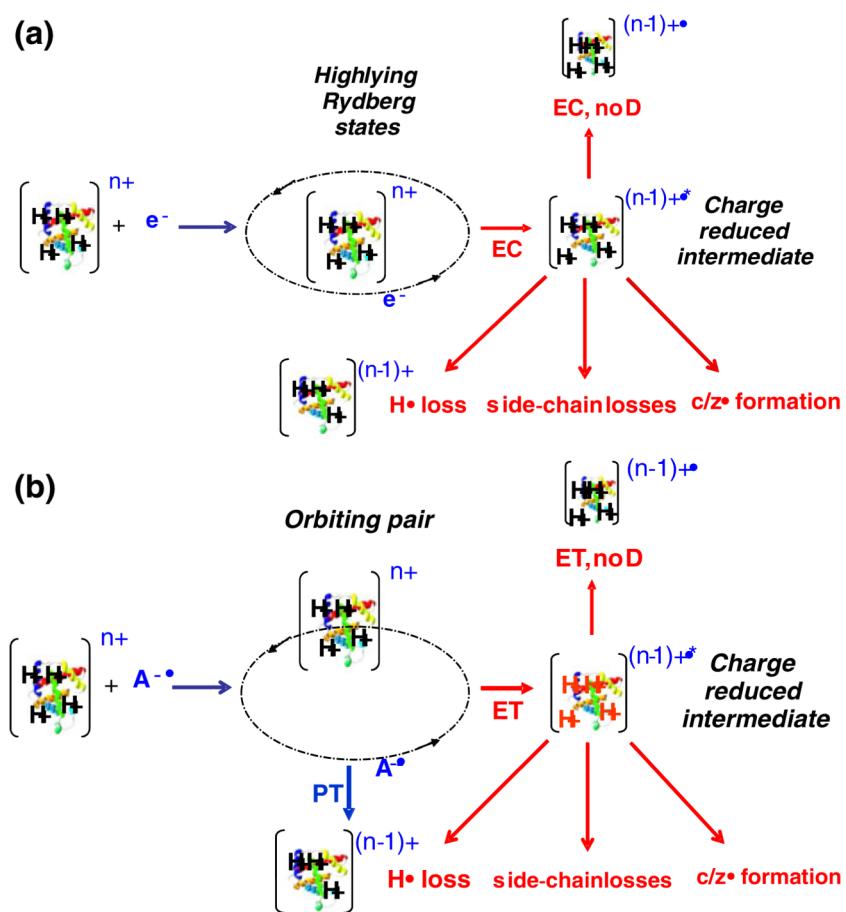
Figure 1.
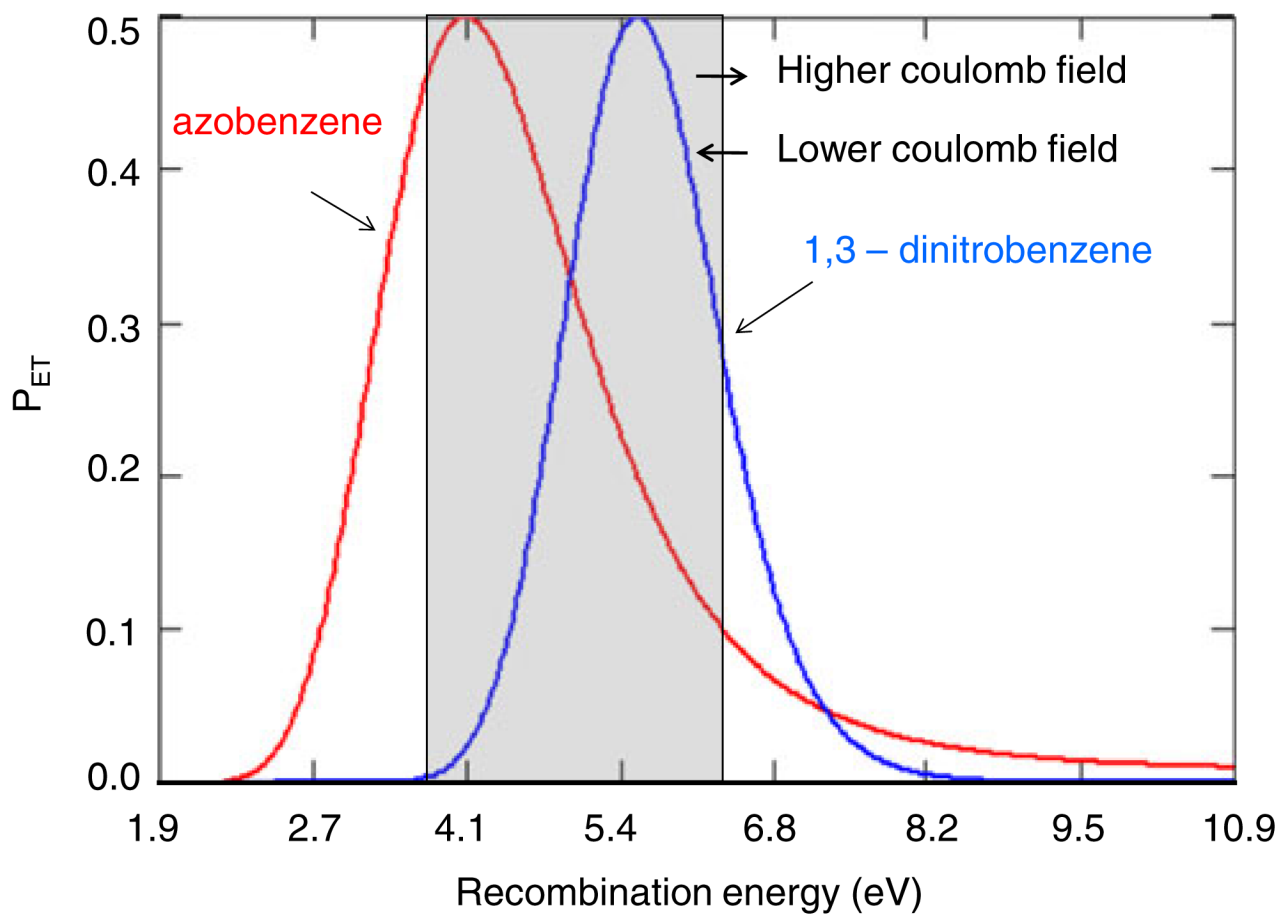Schematic representation of product partitioning in **(a)** ECD and **(b)** ETD

Figure 2.
Plots of P_{ET} for the formation of ground state product cations as a function of cation recombination energy for azobenzene (left-most curve) and 1,3-dinitrobenzene (right-most curve) radical anions generated using the model summarized above. The gray area indicates the range of cation recombination energies likely to apply to the cations in Tables 1, 2, and 3
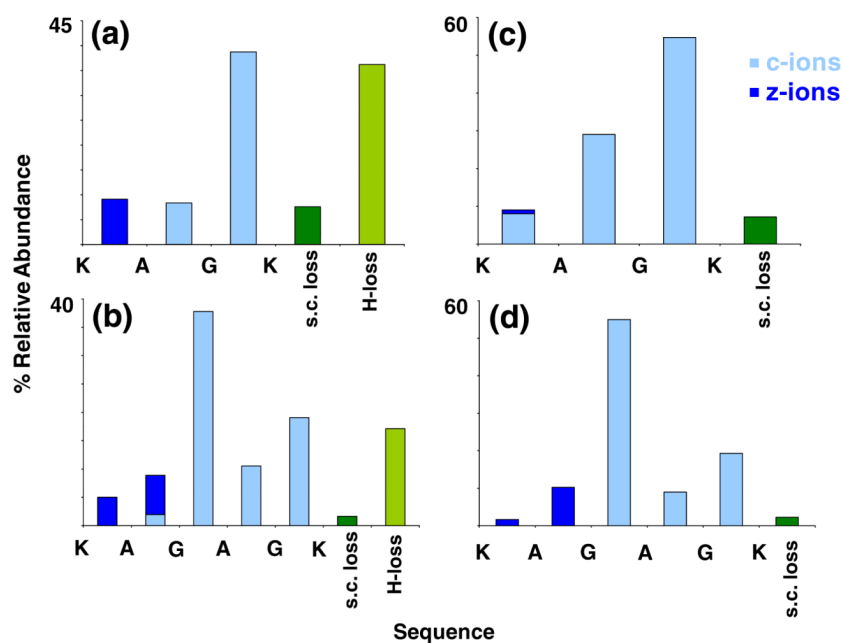
Figure 3.
Relative abundances of product ions resulting from: **(a)** ECD of $[KAGK + 2H]^{2+}$, **(b)** ECD of $[KAGAGK + 2H]^{2+}$, **(c)** ETD of $[KAGK + 2H]^{2+}$, and **(d)** ETD of $[KAGAGK + 2H]^{2+}$
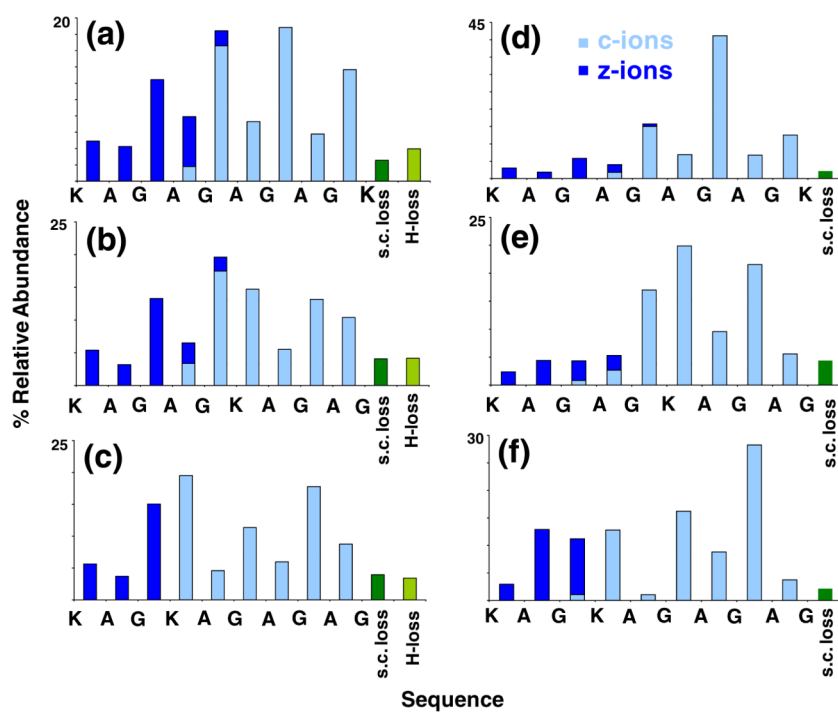
Figure 4.
Relative abundances of product ions resulting from: **(a)** ECD of $[K(AG)_4K + 2H]^{2+}$, **(b)** ECD of $[K(AG)_2K(AG)_2 + 2H]^{2+}$, **(c)** ECD of $[KAGK(AG)_3 + 2H]^{2+}$, **(d)** azobenzene ETD of $[K(AG)_4K + 2H]^{2+}$, **(e)** ETD of $[K(AG)_2K(AG)_2 + 2H]^{2+}$, and **(f)** ETD of $[KAGK(AG)_3 + 2H]^{2+}$
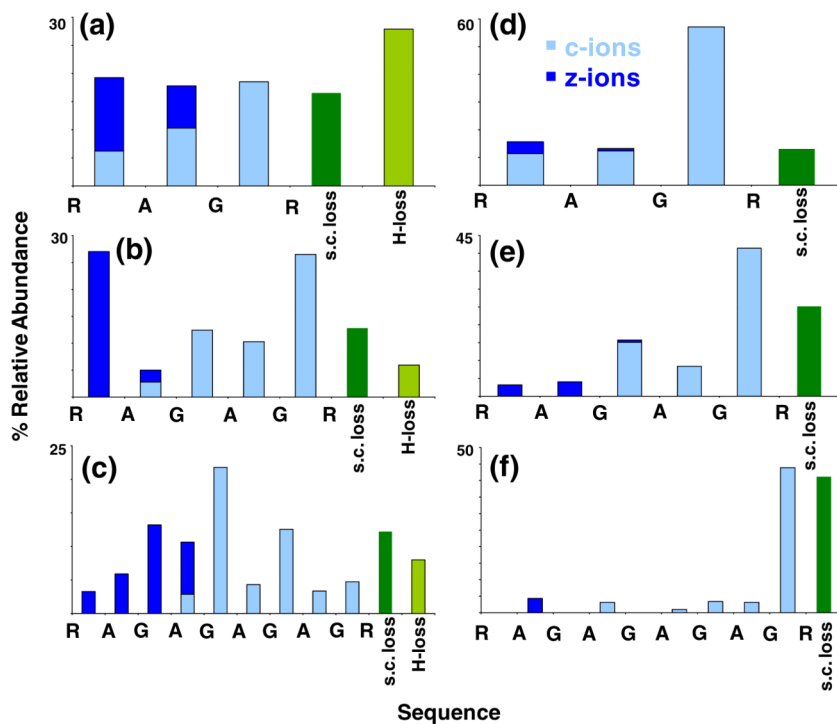
Figure 5.
Relative abundances of product ions resulting from: **(a)** ECD of $[RAGR + 2H]^{2+}$, **(b)** ECD of $[R(AG)_2R + 2H]^{2+}$, **(c)** ECD of $[R(AG)_4R + 2H]^{2+}$, **(d)** ETD of $[RAGR + 2H]^{2+}$, **(e)** ETD of $[R(AG)_2R + 2H]^{2+}$, and **(f)** ETD of $[R(AG)_4R + 2H]^{2+}$
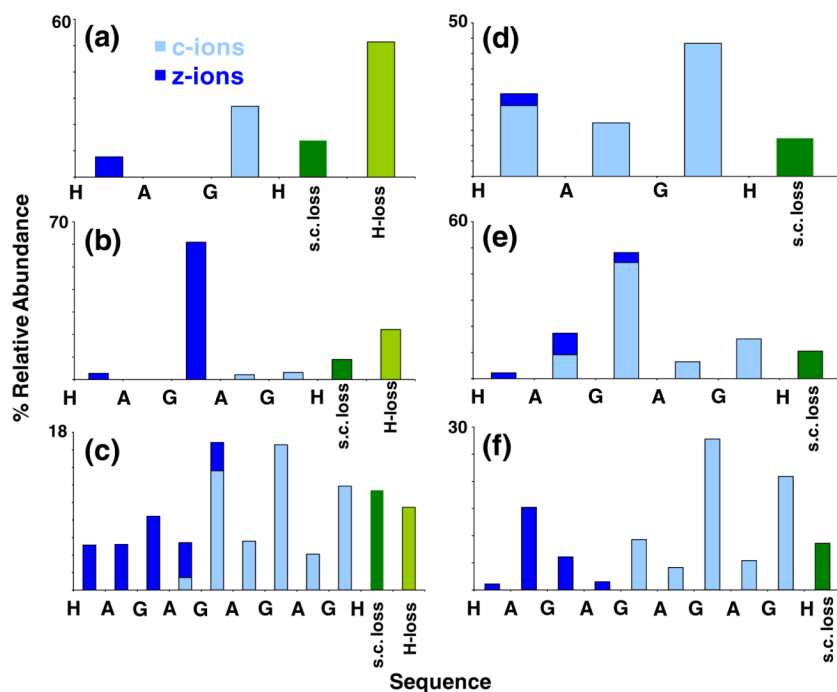
Figure 6.
Relative abundances of product ions resulting from: **(a)** ECD of $[HAGH + 2H]^{2+}$, **(b)** ECD of $[H(AG)_2H + 2H]^{2+}$, **(c)** ECD of $[H(AG)_4H + 2H]^{2+}$, **(d)** ETD of $[HAGH + 2H]^{2+}$, **(e)** ETD of $[H(AG)_2H + 2H]^{2+}$, and **(f)** ETD of $[H(AG)_4H + 2H]^{2+}$

Table 1

Product Ion Partitioning from the Ion/Ion Reactions of Doubly Protonated Peptides with the Radical Anion of Azobenzene

Azobenzene ETD

Row #	Peptide	%	ETD/PT/H• loss	% ET,noD	%PT/H• loss	%c/z•	% side-chain
1	KAGK	100	0		26	69	5
2	KAGAGK	99	1		10	86	4
3	KAGAGAGAGK	98	2		20	78	2
4	KAGAGKAGAG	99	1		21	76	4
5	KAGKAGAGAG	99	1		17	76	7
6	RAGR	100	0		17	62	21
7	RAGAGR	99	1		23	55	22
8	Ac-RAGAGR	95	5		34	39	27
9	RAGAGAGAGR	98	2		48	28	24
10	HAGH	84	16		21	69	10
11	HAGAGH	80	20		27	66	7
12	Ac-HAGAGH	65	35		53	44	3
13	HAGAGAGAGH	83	17		32	62	6

Table 2

Product Ion partitioning from the Ion/Ion Reactions of Doubly Protonated Peptides with the Radical Anion of 1,3-Dinitrobenzene

Row #	**Peptide**	**%ETD/PT/H• loss**	**% ET,noD**	**%PT/H• loss**	**%c/z•**	**% side-chain**
	1,3-Dinitrobenzene ETD					
1	KAGK	100	0	64	35	1
2	KAGAGK	98	2	43	56	1
3	KAGAGAGAGK	97	3	79	21	0
4	KAGAGKAGAG	99	1	76	23	1
5	KAGKAGAGAG	99	1	77	22	1
6	RAGR	100	0	26	62	12
7	RAGAGR	97	3	71	21	8
8	Ac-RAGAGR	100	0	85	10	5
9	RAGAGAGAGR	97	3	91	2	7
10	HAGH	92	8	65	32	4
11	HAGAGH	89	11	85	12	3
12	Ac-HAGAGH	86	14	96	4	0
13	HAGAGAGAGH	93	7	92	7	1

Table 3

Product Ion Partitioning from the Ion/Electron Reactions of Doubly Protonated Peptides with Near-Thermal Electrons

ECD						
Row #	Peptide	%ECD	% EC,noD	H• loss	%c/z•	% side-chain
1	KAGK	100	0	36	57	7
2	KAGAGK	100	0	17	81	2
3	KAGAGAGAGK	100	0	4	93	3
4	KAGAGKAGAG	100	0	4	92	4
5	KAGKAGAGAG	99.9	0.1	3	93	4
6	RAGR	100	0	21	58	21
7	RAGAGR	100	0	12	73	15
8	RAGAGAGAGR	100	0	7	79	14
9	HAGH	100	0	51	35	14
10	HAGAGH	100	0	22	69	9
11	HAGAGAGAGH	86	14	9	79	12